Data in Brief 47 (2023) 108949

Contents lists available at ScienceDirect

Data in Brief

journal homepage: www.elsevier.com/locate/dib

Data Article

Dataset on instrumented Charpy V-notch impact tests of different zones of electron beam welded S960M steel

Raghawendra Sisodia*, Marcell Gáspár

Institute of Materials Science & Technology, University of Miskolc, Miskolc 3515, Hungary

ARTICLE INFO

Article history:
Received 14 November 2022
Revised 16 December 2022
Accepted 30 January 2023
Available online 7 February 2023

Dataset link: Dataset values of Instrumented Charpy V-notch impact tests (ICITs) of base material (BM), heat affected zone (HAZ) and fusion zone (FZ) of the electron beam welded (EBW) joints of S960M high strength (Original data)

Keywords:
Electron beam welding (EBW)
Instrumented Charpy V-notch impact tests
Tensile tests
Optical microscopy
High strength structural steels (HSSS)
$t_{8/5}$ cooling time

ABSTRACT

In this paper, the dataset values of the Instrumented Charpy V-notch impact tests (ICITs) of base material (BM), heat affected zone (HAZ) and fusion zone (FZ) of the electron beam welded (EBW) joints of S960M high strength steel (HSS) of the related article have been presented. This dataset provides the force obtained by the ICITs, which can be used to further plot figures and describes the force (F)-displacement (s) graphs of the individual tested samples of the article. The absorbed impact energy measurements in each sample provide information on the material's behaviour under the impact load. The obtained absorbed impact energy indicates the material's toughness and whether the material failure will be ductile or brittle under impact load. The force-displacement curves from axial tensile loading of S960M specimens are presented. The graphs give information about the highest load and behaviour of load-displacement in axial tensile load testing. In addition, the microstructure images of the base material, fusion zone and different heat-affected subzones were taken by the optical microscopic and are the other parts of the data. ICITs data were collected during in situ impact testing of high strength structural steel S960M using Heckert instrumented impact testing equipment connected to a four-channel digital oscilloscope. A more detailed interpretation of the data presented in this article. The presented data are produced as part of the main work entitled "Experimental

* Corresponding author
E-mail address: raghawendra.sisodia@uni-miskolc.hu (R. Sisodia).

https://doi.org/10.1016/j.dib.2023.108949

assessment of microstructure and mechanical properties of electron beam welded S960M high strength structural steel".

Specifications table

Subject	Mechanical Engineering
Specific subject area	Electron beam welding, High strength structural steel
Type of data	Table Image Graph
How data were acquired	Instrumented Charpy V-notch impact test (ICITs), Heckert instrumented impact testing equipment with Tektronix TDS 2024B digital signal oscilloscope 200 MHz. Tensile tests were performed with ZD 100 (1000 kN) hydraulic materials testing equipment. Optical microscope, microstructure images were taken by using an Axio Observer D1m (Zeiss) inverted microscope.
Data format	Raw Analysed
Parameters for data collection	- For ICITs test, samples were tested at low temperatures (-40°C) - Tensile test was executed at room temperature. - For Optical Microscopic analysis, Magnification, M=200x, M=500x
Description of data collection	- Impact strength value on the scale was recorded after the breaking of the sample due to impact loading. ICITs data are collected in excel file for each tested specimen through digital oscilloscope attached with Heckert impact testing equipment. - Tensile test was plotted on graph paper in situ and further data for graph plot was obtained by digitization. - Optical microscopy was performed on the sample sectioned through the weld in transverse direction and then specimens etched with Nital (2% HNO_3) for 10 s.
Data source location	Institute of Materials Science & Technology; University of Miskolc Miskolc, Borsod Abaúj Zemplén, 3515 Hungary
Data accessibility	Repository name: Mendeley Data Data identification number: 10.17632/p4dmsb9rxr.1 Direct URL to data: https://data.mendeley.com/datasets/p4dmsb9rxr
Related research article	R.P.S. Sisodia, M. Gáspár, Experimental assessment of microstructure and mechanical properties of electron beam welded S960M high strength structural steel, Manufacturing Letters, Vol. 29, pp. 108-112, 2021, https://doi.org/10.1016/j.mfglet.2021.05.004

Value of the Data

- These data can be used further to compare the behaviour of the material under impact loading, tensile test results, microstructural analysis and $t_{8/5}$ cooling time with same grade high strength steel welded joint with different welding processes or higher strength steel grades welded joint with gas metal arc welding (GMAW) or other welding processes.
- Researchers, structural engineers, modelling engineers, crane and lifting process industries etc. will benefit from these data. These EBW joint test data will help in comparisons with other welding processes like GMAW, laser hybrid, plasma etc., as well as their interactions in HSS like S960M.
  ICITs data can be used to correlate its test results with the result of static tensile testing (analysis of the maximum force, yield forces at Charpy instrumented method and the

static tensile test), analytical cooling time determination will help in numerical simulation of EBW process and its comparative analysis.
- The tensile test data (F_{max}) can be used to compare with tensile behavior of other welding process joints of the same grade, validate and calibrate future numerical modelling of tensile strength analysis.

1. Objective

The primary goal of this data article is to provide detailed supplementary experimental process, analytical cooling time determination information, tensile test data, Instrumented Charpy V-notch tests (ICITs), and an optical microstructure picture in support of the published article. Because the published articles only offer the most essential and noteworthy results, this dataset contains extra experimental process information as well as images to benefit readers. The images and graphs of tensile testing and fractured specimens will add extra worth to the paper. At -40°C, the ICIT detail analysis is shown for each of the investigated samples (number of samples for BM, FZ, and HAZ = 5 each). The ICITs' examined data include information on the maximum force ($F_{max.}$) at crack initiation (W_i), and crack propagation (W_p) energies, which are important for showing the proportion of energy involved in W_i and W_p, as well as the ductile-brittle behaviour of the material. The graphs of each ICIT's fractured samples were analyzed and presented in a force-displacement diagram, which gives detailed information and characteristic graphs for BM, FZ, and HAZ. These ICITs test results give the reader more information to compare with fracture toughness.

2. Data description

The data provided in this paper is related to the paper submitted in Manufacturing Letters [1]. Fig. 7(a) and Fig. 7(b) show the EB-welding set-up in a vacuum chamber and the not through penetration mode [2] respectively. The details of the beam oscillation used in this experiment are shown in the schematic diagram in Fig. 8. The optimal welding parameters used in this investigation are shown in Table 2 [3]. Fig. 1a. shows the different positions on the welded joint where micrographs are taken. Fig. 1b and Fig. 1c show the microstructures of the S960M base material and fusion zone, respectively. The different sub-zones of the heat-affected zone, i.e., coarse-grained heat-affected zone (CGHAZ), fine-grained heat-affected zone (FGHAZ) and the intercritical heat-affected zone (ICHAZ) are shown in Fig. 1d, Fig. 1e and Fig. 1f respectively. The schematic view of the transverse tensile specimen with dimensions is given in Fig. 9. The force-displacement curves of the two samples with maximum forces for the EB- welded joints are shown in Fig. 2. The macroscopic photos of the fractured surfaces of both samples 1 and 2 are shown in Fig. 3. The standard dimensions and incised position in the specimens are illustrated in Fig. 10a. and Fig. 10b. Table 1 shows the CVN values of the real EB welded joints made of the investigated S960M material, along with the average (Avg.) CVN, standard deviation (Std. Dev.) CVN, where, W_i is the absorbed energy during crack initiation, W_p is the absorbed energy during crack propagation.

The dataset used for plotting Force (F)- displacement (s) graphs in Fig. 4(a-e), Fig. 5(a-e), and Fig. 6(a-e) are provided with the research data (.CSV file) along with this article. The file number of the excel sheet for each tested specimen is mentioned in Table 1. Column D & E of the raw data in the excel sheets represent the time (s) & F (V) obtained from ICITs, respectively.

The development of higher grades TMCP steel and the requirements for welded structures have prompted extensive study into the characteristics influencing the behavior of these materials in structures during welding and after-weld operation [4,5,6,7]. The characteristic features of high strength structural steels like S960M are make them exceptional for application in the field of engineering structures and highly loaded constructional components like heavy duty trucks, cranes, bridges, mobile cranes, etc. [3,8,9,10].

2.1. Microstructure

The metallographic samples for optical micrography observations were sectioned through the weld in a transverse direction. The sectioned samples were polished with SiC waterproof papers in series of 120, 400, 800 & 2000 ANSI grit and finally with a disc using diamond paste of

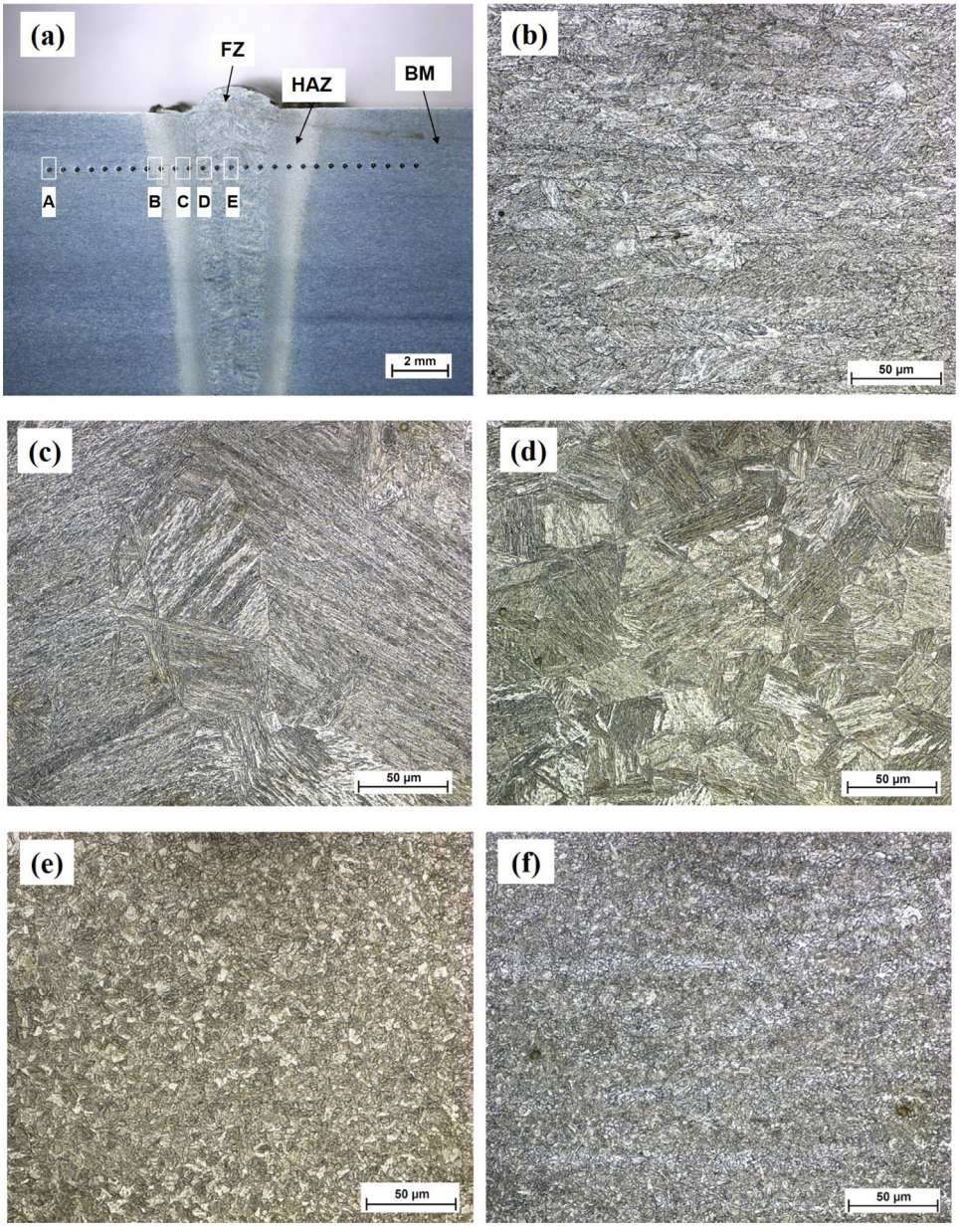

Fig. 1. Microstructures S960M: (a) Microscopy position, (b) BM [A], (c) FZ [E], (d) CGHAZ [D], (e) FGHAZ [C], and (f) ICHAZ [B]; M=500x.

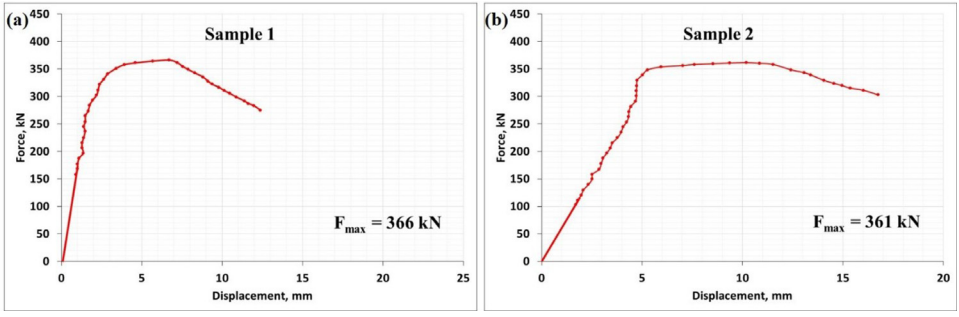

Fig. 2. Force-displacement graph of S960M specimens.

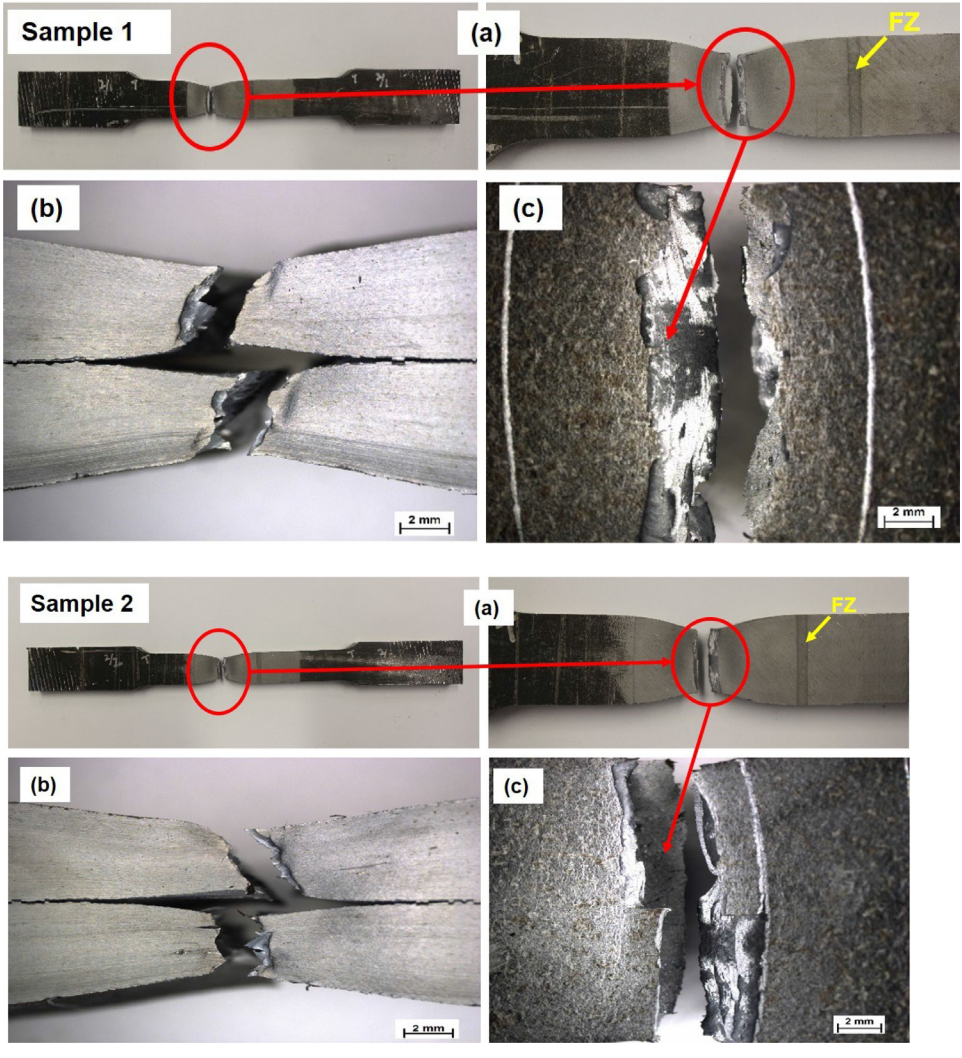

Fig. 3. Tensile tests fractured specimen: S960M; Sample 1 and Sample 2.

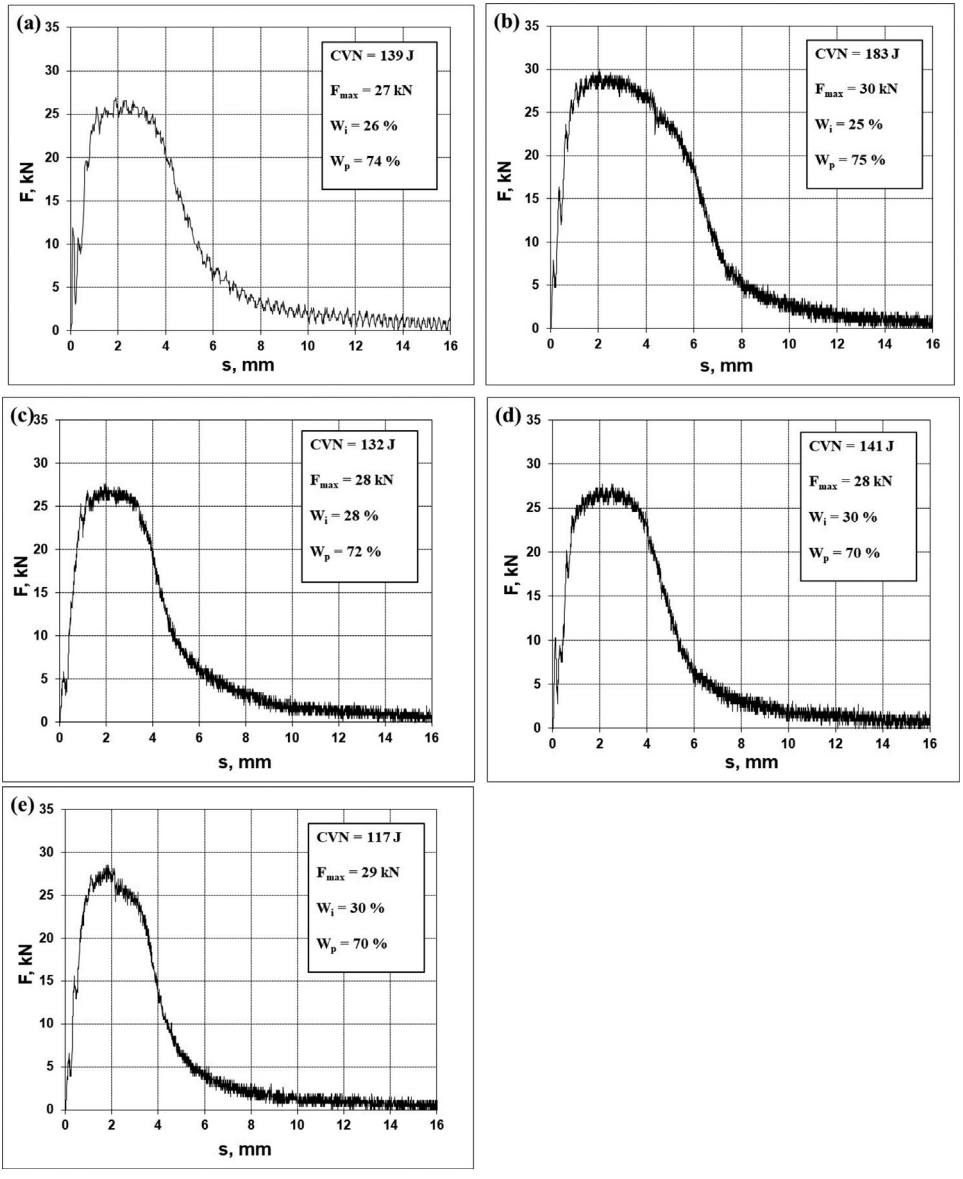

Fig. 4. (a-e). Instrumented Charpy V-notch test, Force-displacement graph, Base material.

1 µm [1,11]. The specimens were then etched with Nital (2% HNO_3) for 10 s to observe the microstructure of base materials and weld materials. The micrograph position in the welded joint and the resulting image of optical microscopy (M=500x) of S960M base material are shown in Fig. 1a and Fig. 1b, respectively. The microstructure of the as-received, S960M base material is composed of upper bainite and martensite, as shown in Fig. 1b.

Optical micrographs of the fusion zone (FZ) and heat-affected zones (HAZ) of S960M EBW joints are shown in Fig. 1c and Fig. 1d, Fig. 1e & Fig. 1f respectively. The S960M fusion zone reveals that it consists of mainly martensitic microstructure, which is clearly observed in Fig. 1c.

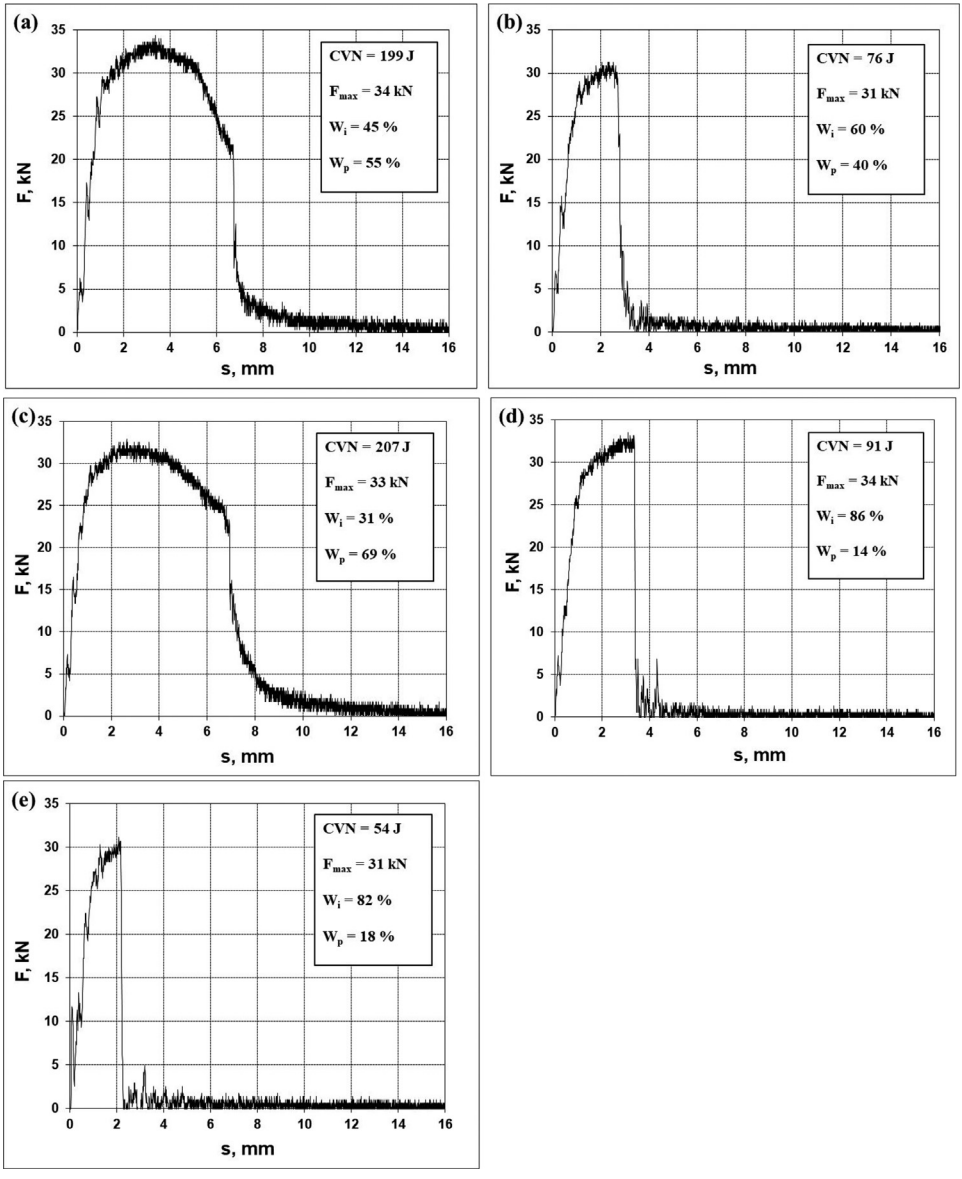

Fig. 5. (a-e). Instrumented Charpy V-notch test, Force-displacement graph, Heat-affected zone.

2.2. Tensile properties

The force- displacement curves of the two samples with maximum forces for the EB-welded joints are shown in Fig. 2. The macroscopic photos of fractured surfaces of both samples 1 and 2 are shown in Fig. 3. The photos (Fig. 3a) of sample 1 & sample 2 clearly show that the fractures occurred in the base metal and not in the weld.

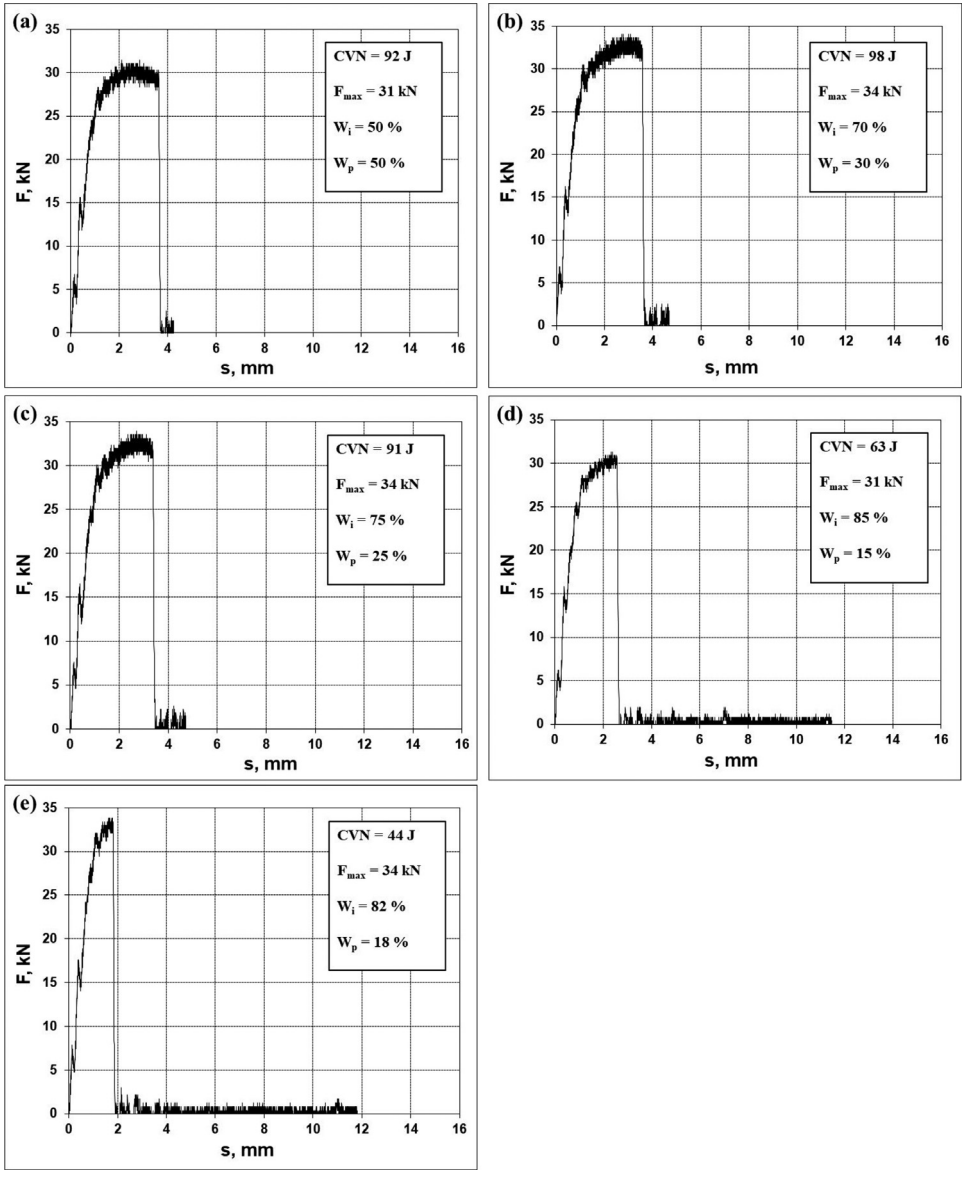

Fig. 6. (a-e). Instrumented Charpy V-notch test, Force-displacement graph, Fusion zone.

2.3. Instrumented Charpy V-notch impact test details

In the ICITs test, 5 samples were used to evaluate the impact energy for BM, HAZ, and FZ to obtain a more precise average estimate of the impact energy. However, the standard requires a minimum of three samples [12,13]. The original file name (.CSV) of each examined specimen is given in Table 1, and the files are included with the research data that comes with this dataset article. These research data files include the information gathered during ICITs.

Table 1
Measured CVN values of EB welded S960M joints.

Zone	Measured Charpy V-notch test values of EB welded S960M joints										
	S. No.	File No.	Fig. No.	CVN, J	CVN (J), Avg.	CVN (J), Std. Dev.	F_{max}, kN	W_i; J, (%)	W_i (%), Std. Dev.	W_p; J, (%)	W_p(%), Std. Dev.
BM	**1**	TEK0002.CSV	Fig. 4a	139	142	22	27	36(26)	2	103(74)	2
	2	TEK0004.CSV	Fig. 4b	183			30	46(25)		137(75)	
	3	TEK0017.CSV	Fig. 4c	132			28	37(28)		95(72)	
	4	TEK0018.CSV	Fig. 4d	141			28	42(30)		99(70)	
	5	TEK0019.CSV	Fig. 4e	117			29	35(30)		82(70)	
HAZ	**1**	TEK0012.CSV	Fig. 5a	199	125	64	34	90(45)	21	109(55)	21
	2	TEK0006.CSV	Fig. 5b	76			31	46(60)		30(40)	
	3	TEK0009.CSV	Fig. 5c	207			33	64(31)		143(69)	
	4	TEK0011.CSV	Fig. 5d	91			34	78(86)		13(14)	
	5	TEK0015.CSV	Fig. 5e	54			31	44(82)		10(18)	
FZ	**1**	TEK0025.CSV	Fig. 6a	92	78	21	31	46(50)	12	46(50)	12
	2	TEK0026.CSV	Fig. 6b	98			34	69(70)		29(30)	
	3	TEK0027.CSV	Fig. 6c	91			34	68(75)		23(25)	
	4	TEK0022.CSV	Fig. 6d	63			31	54(85)		9(15)	
	5	TEK0023.CSV	Fig. 6e	44			34	36(82)		8(18)	

(Abbreviation details: CVN, J- Charpy V-notch impact energy, Joule; $F_{max.}$ (kN)- Maximum force, kilo Newton; W_i, J- The absorbed energy for crack initiation, Joule; W_p, J- The absorbed energy for crack propagation, Joule; Avg.- Average; Std. Dev.- Standard Deviation; (%)- Percentage of energy)

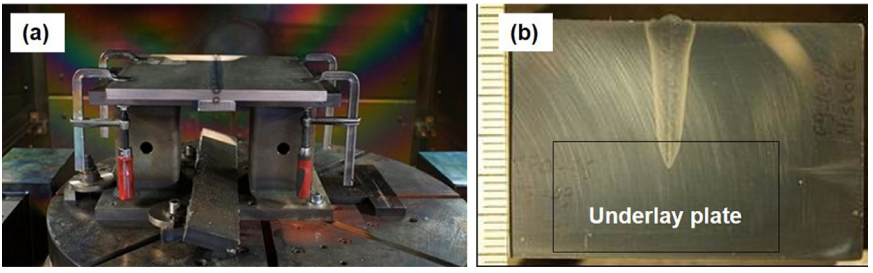

Fig. 7. (a) EBW welding set-up in vacuum chamber (b) Not through penetration mode.

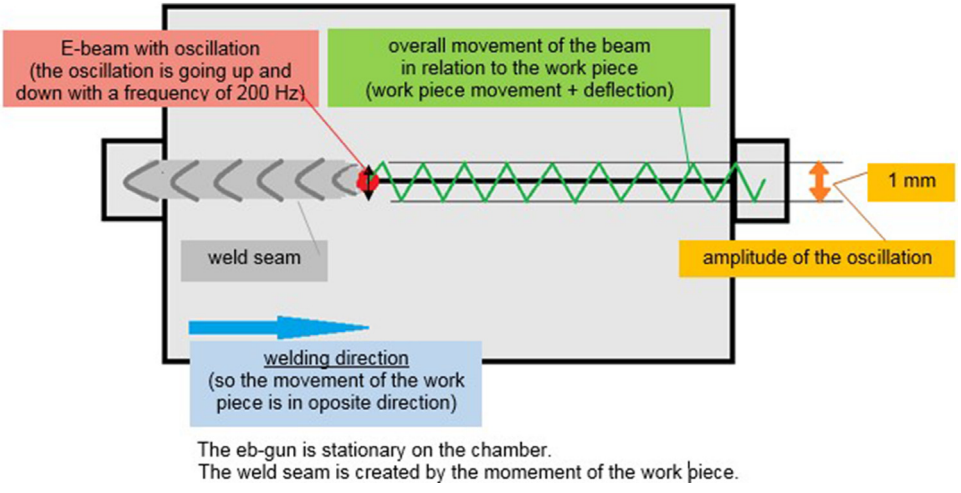

Fig. 8. Schematic of beam oscillation, EBW of S960M welded joint.

In Table 1, the CVN values of the real EB welded joints from the investigated S960M material are presented with average (Avg.) CVN, standard deviation (Std. Dev.) of CVN.

The load-time graph was generated using the instrumented CVN test with strain gauge and a digital signal oscilloscope. The force-displacement graph was also developed for each individual tested specimen based on the load-time graph. Fig. 4(a-e), Fig. 5(a-e), and Fig. 6(a-e) show the load (F)-displacement (s) graphs for each instrumented Charpy V-notch test for BM, HAZ, and FZ, respectively.

3. Experimental design, materials and methods

In this experiment, base material (BM) namely ALFORM (S960M) [14] with a plate thickness 15 mm was used. The chemical composition and mechanical properties are presented in the article [1]. The plates with dimensions 300 mm × 150 mm × 15 mm (according to EN 15614-11:2002) in two pieces for the butt welded joint were used under a high vacuum of 2×10^{-4} mbar for electron beam welding using an EBOCAM EK74C–EG150-30BJ EBW machine shown in Fig. 7(a) The electron beam welding process is an innovative and versatile technology [15]. The underlay plate with dimension of 300 × 50 mm was used for EBW process with not through penetration mode Fig. 7(b) to obtain sound result, assembled with original butt welded joint.

The edges of the samples and assembly unit of backing plate with butt joint plates were properly cleaned and milled to the maximum allowable gap of 0.15 mm. The electron beam

Table 2
Optimal EBW welding parameters based on preliminary experiments.

Steels	Accelerating voltage (kV)	Beam current (mA)	Welding speed (mm/s)	Beam diameter (mm)	Working distance (mm)
S960M	150	49	10	0.4	500

welded joint without filler material with full penetration was obtained after several trials and the beam pattern was straight oscillation with the amplitude of 1 mm.

The linear heat input was calculated using Eq. 1 [16,17] with parameters provided in Table 2. and efficiency (η= 0.9) [10] as 0.661 kJ/mm.

$$Q = \eta \frac{V_a I_b}{s} \tag{1}$$

3.1. Cooling time ($t_{8/5}$) determination

The cooling time determination is very important because the microstructural changes in the welded joint and heat affected zone (HAZ) depends on it and further it influences the steels mechanical properties. The cooling time $t_{8/5}$ (3D) is described by the following equation for the three-dimensional heat flow for thick plate [17]:

$$t_{8/5(3D)} = \frac{1}{2\pi k} Q\left[\left(\frac{1}{500 - T_0}\right) - \left(\frac{1}{800 - T_0}\right)\right] \tag{2}$$

Q= 661.5 J/mm, η= 0.9 (EBW) [10], k= 0.0378 J/ (mm.s.K) [18], T_0= 21°C where,

$t_{8/5}$ (3D) = 3D cooling time from 800°C to 500°C (s)
k= thermal conductivity (J/ (s.mm.K))
Q= linear heat input (J/mm)
T_o= plate initial temperature (°C)

The calculated cooling time from the abovementioned data using Eq. 2 is 2.23 s. The lower ($t_{8/5}$ < 5 s) cooling time (energy input) than arc welding is usual and characteristic of the electron beam welding process. The $t_{8/5}$ depends on energy input which includes the welding speed, welding voltage, welding current and thermal efficiency. Higher the energy input more will be the $t_{8/5}$ cooling time. Higher the preheating temperature and interpass temperature greater will be the $t_{8/5}$ time.

3.2. Tensile properties

The tensile test was executed with a ZD 100 (1000 kN) hydraulic materials testing equipment at room temperature, and the specimens used for mechanical tests were designed according to the ISO 4136:2012 standard. The specimens were milled and etched prior to tensile tests in order to view FZ & HAZ from the welded sheets and see the fracture along the welded specimens. The transverse (perpendicular to welding direction) tensile tests were performed on EB welded specimens (S960M, 15 mm thickness) and the ultimate tensile strength of all welded specimens has been determined. The schematic view of the transverse tensile specimen with dimensions is given in Fig. 9.

The force- displacement curves of the two samples with maximum forces for the EB-welded joint was plotted on graph paper in situ during testing and further data for graph plot was obtained by digitization.

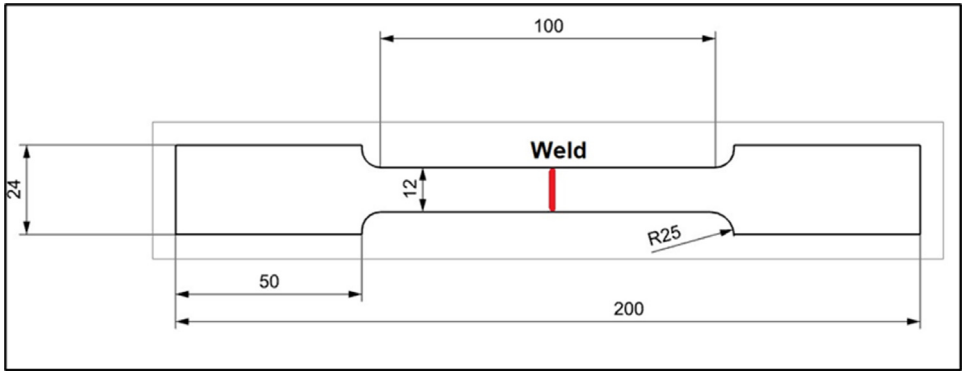

Fig. 9. Schematic sketch of the tensile test specimen

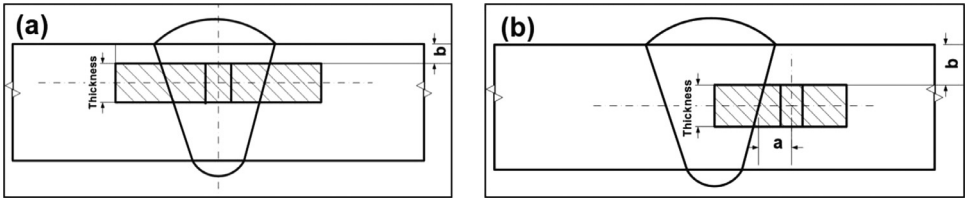

Fig. 10. Charpy V test specimen sizes per EN ISO 9016:2011. a VWT; V-notch in fusion zone. b VHT; V-notch in HAZ (All dimensions in mm).

3.3. Instrumented Charpy V-notch impact tests

Instrumented Charpy V-notch impact tests were done by Heckert instrumented impact testing equipment connected with a digital oscilloscope in accordance with EN ISO 14556 standards to evaluate the impact toughness of BM, HAZ, FZ. Specimens incised in the FZ are marked VWT and specimens incised in the HAZ are marked VHT. The standard dimensions and incised position in the specimens are illustrated in Fig. 10a. and Fig. 10b. In Fig. 10a & Fig. 10b, notation "a" is the distance of the centre of the notch from the reference line; a= 0.75 mm & "b" is the distance from the weld joint face side to the nearest face of the test specimen; b= 3 mm. At -40°C temperature, the Charpy V-notch impact test was used to determine whether the material is brittle or ductile.

Five Charpy V-notch specimens with dimensions of 10 × 10 × 55 mm at -40°C for BM, HAZ and FZ were tested. With the application of the strain gauge measurement technique, the load-time graph was obtained, and the characteristic points of the fracture process were identified (the start of the plastic strain, the maximal force, the start of the unstable crack propagation, and the end of the unstable crack propagation). From the load-time graph, the force-displacement graph was calculated. Considering that crack initiation occurs at the maximal force, the registered graph was divided into two parts according to the maximal force. Until the maximum force, the area under the curve was considered the absorbed energy for crack initiation (W_i), and the rest for crack propagation (W_p). The fracture surfaces of the tested samples (whose average value is nearest among the 5 tested samples) obtained for BM, FZ & HAZ and examined via a SEM equipped with three-dimensional (3D) fractographic imaging analysis are shown in Fig. 3a, Fig.3b & Fig. 3c respectively [1].

Ethics Statements

The research work does not involve studies with humans and animals as subjects, and the data were not collected from social media platforms.

Declaration of Competing Interest

The authors declare that they have no known competing financial interests or personal relationships which have or could be perceived to have influenced the work reported in this article.

Data availability

Dataset values of Instrumented Charpy V-notch impact tests (ICITs) of base material (BM) , heat affected zone (HAZ) and fusion zone (FZ) of the electron beam welded (EBW) joints of S960M high strength (Original data) (Mendeley Data).

CRediT Author Statement

Raghawendra Sisodia: Methodology, Data curation, Writing – original draft, Conceptualization, Visualization, Investigation; **Marcell Gáspár:** Writing – review & editing.

Acknowledgments

This research was supported by the European Union and the Hungarian State, co-financed by the European Regional Development Fund in the framework of the GINOP-2.3.4-15-2016-00004 project. The authors wish to express their appreciation to Steigerwald Strahltechnik GmbH, Maisach, Germany (www.sst-ebeam.com) for the production of electron welded joints.

References

[1] R. Sisodia, M. Gáspár, Experimental assessment of microstructure and mechanical properties of electron beam welded S960M high strength structural steel, Manuf. Lett. (2021), doi:10.1016/j.mfglet.2021.05.004.
[2] H Schultz, Electron Beam Welding, Abington Publishing, Cambridge, 1993.
[3] R.P.S. Sisodia, High Energy Beam Welding of Advanced High Strength Steels, University of Miskolc, 2021 PhD Thesis.
[4] J. Gorka, Weldability of thermomechanically treated steels having a high yield point, Arch. Metall. Mater. 60 (2015) 469–475, doi:10.1515/amm-2015-0076.
[5] J. Gorka, T. Poloczek, A. Kotarska, W. Jamrozik, Analysis of precipitates in heat treated thermo- mechanically processed steel with a high yield strength, IOP Conf. Ser. Mater. Sci. Eng. (2021), doi:10.1088/1757-899X/1182/1/012026.
[6] M. Tümer, F. Pixner, R. Vallant, J. Domitner, N. Enzinger, Mechanical and microstructural properties of S1100 UHSS welds obtained by EBW and MAG welding, Weld. World. (2022), doi:10.1007/s40194-022-01276-7.
[7] A. Lisiecki, Development of laser welding and surface treatment of metals, Materials (Basel) 15 (2022), doi:10.3390/ma15051765.
[8] M. Błacha, S Węglowski, M.S. Dymek, S. Kopuściański, Microstructural and mechanical characterization of electron beam welded joints of high strength S960QL and WELDOX 1300 steel grades, Arch. Met. Mater. 62 (2017) 627–634, doi:10.1515/amm-2017-0092.
[9] K. Májlinger, E. Kalácska, P.Russo Spena, Gas metal arc welding of dissimilar AHSS sheets, Mater. Des. 109 (2016) 615–621, doi:10.1016/j.matdes.2016.07.084.
[10] W. Maurer, W. Ernst, R. Rauch, S. Kapl, A. Pohl, T. Krüssel, R. Vallant, N. Enzinger, Electron beam welding of a TMCP steel with 700 MPa yield strength, Weld. World. 56 (2012) 85–94, doi:10.1007/BF03321384.
[11] G. Vander Voort,Metallography and Microstructures, ASM International, 2004, doi:10.31399/asm.hb.v09.9781627081771.
[12] EN ISO 15614-1: 2017, Specification and qualification of welding procedures for metallic materials — Welding procedure test — Part 1: Arc and gas welding of steels and arc welding of nickel and nickel alloys.
[13] ASTM A673/A673M-07, Standard specification for sampling procedure for impact testing of structural steel.
[14] J. Lukács, Fatigue crack propagation limit curves for high strength steels based on two-stage relationship, Eng. Fail. Anal. 103 (2019) 431–442, doi:10.1016/j.engfailanal.2019.05.012.

[15] M.S. Węglowski, S. Błacha, A. Phillips, Electron beam welding - Techniques and trends - Review, Vacuum 130 (2016) 72–92, doi:10.1016/j.vacuum.2016.05.004.
[16] S. Kou, Welding Metallurgy, 2nd ed., A John Wiley & sons, Inc., 2002.
[17] B.K.-H. Chan, Software for Welding Engineers (1990) Thesis.
[18] M. Gáspár, Physical Simulation Based Development Of Welding Technology For Quenched And Tempered Structural High Strength Steels, University of Miskolc, 2016 PhD Thesis.